

GDP nowcasting with artificial neural networks: How much does long-term memory matter?

Kristóf Németh*, Dániel Hadházi†

Abstract

In our study, we apply different statistical models to nowcast quarterly GDP growth for the US economy. Using the monthly FRED-MD database, we compare the nowcasting performance of the dynamic factor model (DFM) and four artificial neural networks (ANNs): the multilayer perceptron (MLP), the one-dimensional convolutional neural network (1D CNN), the long short-term memory network (LSTM), and the gated recurrent unit (GRU). The empirical analysis presents the results from two distinctively different evaluation periods. The first (2010:Q1 – 2019:Q4) is characterized by balanced economic growth, while the second (2010:Q1 – 2022:Q3) also includes periods of the COVID-19 recession. According to our results, longer input sequences result in more accurate nowcasts in periods of balanced economic growth. However, this effect ceases above a relatively low threshold value of around six quarters (eighteen months). During periods of economic turbulence (e.g., during the COVID-19 recession), longer training sequences do not help the models' predictive performance; instead, they seem to weaken their generalization capability. Our results show that 1D CNN, with the same parameters, generates accurate nowcasts in both of our evaluation periods. Consequently, first in the literature, we propose the use of this specific neural network architecture for economic nowcasting.

Keywords: GDP nowcasting, Artificial neural networks, 1D CNN, Long-term memory
Journal of Economic Literature (JEL) codes: C45, C53, C51

1 Introduction

Gross domestic product (GDP) is the market value of all final goods and services made within a country during a specific period. GDP is arguably the most important flow-type monetary

*Corresponding author. Faculty of Electrical Engineering and Informatics, BME, manzotta@gmail.com

†Department of Measurement and Information Systems, BME, hadhazi@mit.bme.hu

measure of economic activity over a given period. GDP is typically calculated on an annual basis, but in most market economies it is also measured on a quarterly frequency. Considering its relevance, the availability and reliability of these quarterly data are of great significance.

However, due to the time required for data collection and statistical data processing, statistical offices are delayed in releasing GDP data for the current quarter. The first measurements are usually available only a few months after the end of the current quarter, which makes it difficult to assess economic activity in real-time (i.e., synchronously). Therefore, many decision makers (such as central banks, budget offices, etc.) rely on the current quarter forecast, that is, the nowcast of GDP growth for more informed policy making. This underscores the need for accurate nowcasts.

In nowcasting current quarter GDP growth, one typically tries to extract the informational content of higher frequency monthly data to track the real-time development of economic activity. Such an analysis faces the following three problems (Giannone et al., 2008): (i) Combining monthly predictor variables and a quarterly target variable. (ii) Handling a large number of potential regressors. (iii) Monthly data are released at different times (unsynchronized) within a quarter. This leads to the so-called “*ragged edge*” problem, where some monthly features may have missing values, usually at the end of the sample period (Wallis, 1986).

In our study, we apply different statistical models to nowcast the quarterly U.S. GDP growth of the current quarter. Using the monthly FRED-MD database, we measure the nowcasting performance of the dynamic factor model (DFM) and four different artificial neural networks (ANNs) relative a naive constant growth model. These methods are similar in that they all try to meet the above-mentioned challenges of nowcasting. However, the models have a different structure. As far as classical statistical modeling goes, DFM is widely considered as the state-of-the-art modeling framework. In the course of the empirical analysis, we adopt four different ANN architectures: the multilayer perceptron (MLP), the one-dimensional convolutional neural network (1D CNN), the long short-term memory network (LSTM), and the gated recurrent unit (GRU). Our results indicate that some ANNs can outperform the dynamic factor model in terms of out-of-sample nowcasting performance, while others cannot.

The first main contribution of our study is that it proposes the utilization of a neural network architecture that has not yet been applied for economic nowcasting, namely the one-dimensional convolutional neural network (hereinafter, 1D CNN). Our results suggest that the 1D CNN could be a highly suitable architecture for GDP nowcasting as it generates accurate nowcasts for both evaluation periods, i.e., both during a balanced growth period and in times of high economic turbulence.

While this ANN architecture has been neglected compared to MLP and the more modern gated RNNs, we argue that it represents a “*sweet spot*” for this type of analysis in many aspects. In contrast to the MLP, 1D CNN has an intrinsic architectural constraint that usefully limits the hypothesis space, i.e., the range of mappings the network can learn during the training process. During training, the network learns the coefficients of different finite impulse response filters, so it can only learn time-invariant (translation-invariant) mappings. Intuitively, the network performs a series of hierarchical pattern recognition tasks where the result is time-invariant with respect to the relative position of those patterns (Goodfellow et al., 2016). It is worth noting that the DFM, and the majority of the traditional time series approaches are also built around this assumption; namely, the conditional distribution of the target variable only depends on time through the regressors (predictors). Consequently, it seems especially advantageous to narrow the hypothesis space to this type of mappings. Unlike the MLP, 1D CNN is trained with input sequences, reflecting the architecture’s temporal “awareness”. In this regard, MLP is the exception here: While we can form “training sequences” by hand, the MLP does not recognize the natural temporal ordering in the data. Thus, training of the MLP cannot make use of this type of regularity either. Compared to the other three networks investigated in this paper, MLP is a simple, time-agnostic architecture which is not tolerant to shifts (translations) in time (Ekman, 2021, Goodfellow et al., 2016).

In our study, we investigate two types of gated RNNs: the long short-term memory network (LSTM) and the gated recurrent unit (GRU). Both of these architectures also reflect an explicit temporal aspect, i.e. they are trained with input sequences, and possess a time-invariant property as well. In fact, they are more flexible and complex compared to the 1D CNN: They can be trained with much longer and even variable-length input sequences. This type of flexibility and complexity comes at a cost however, since gated RNNs have much more trainable parameters than 1D CNNs – even in their simplest form (Ekman, 2021, Goodfellow et al., 2016). The results from the second evaluation period indicate that this trade-off clearly favors the 1D CNN: Its more restricted architecture results in a smaller hypothesis space and ultimately more accurate nowcasts during sharp changes in economic growth.

The second main contribution of the paper is that it presents the results of a nowcasting competition focusing on the performance of different ANN architectures. We believe that the results from two distinctively different evaluation periods provide a better understanding of the underlying data-generating process.

The major novelty of gated RNNs is that they introduce a so-called *gating mechanism* (practically, element-wise multiplication) that enables the network to develop long-term memory. This

feature helps to overcome the vanishing gradient problem of the vanilla RNNs, making them a much more viable option for modeling time series with path-dependent behavior i.e., with long-term memory (Chung et al., 2014, Hochreiter and Schmidhuber, 1997). Financial time series, such as stock prices or foreign exchange rates, generally show characteristics of path-dependency (e.g., a slowly decaying autocovariance function). Here, it can easily happen that the current value of the exchange rate is affected (supported) by a distant technical level whose effect, however, is no longer reflected in any nearby values. As a result, this old technical level should be remembered by the network in a predictive exercise. We try to answer, how important long-term memory is in modeling GDP growth? If the unobserved data generation process of GDP growth was actually path-dependent, than that would speak for the use of gated RNNs in almost any predictive scenario. Due to the gating mechanism, their architecture supports the modeling of path-dependent (long-term memory) processes much better than the MLP or the 1D CNN.

The first evaluation period ranges from 2010:Q1 to 2019:Q4, so it ends before the economic consequences of the COVID-19 pandemic would hit the economy. The results for this period suggest that economic growth can be better modeled in normal times based on longer input sequences and more refined network architectures. While gated RNNs provide the most accurate nowcasts for this period, 1D CNN comes close in terms of both RMSE and MAE evaluation. Our second evaluation period is from 2010:Q1 to 2022:Q3, so it also includes the COVID-19 crisis. Under such circumstances, MLP comes out on top with its simple time-agnostic architecture. According to the results, shorter input sequences generally result in more accurate nowcasts. Here we see again that 1D CNN with eight-month-long sequences comes close to the best performing model in terms of both RMSE and MAE. This time, however, architectural complexity does not help the gated RNNs' nowcasting performance in any meaningful way. Combined results from the two evaluation periods show that longer input sequences do not improve our models' predictive accuracy. That is especially interesting to see in the case of the LSTM and the GRU: While their architectural design enables them to handle long input sequences, forming a long-term memory, even these networks tend to have better accuracy with shorter sequences. Considering the results from the two test periods as a whole, GDP growth could be approximated as a well-behaved ergodic time series – at least for prediction purposes.

The remainder of the paper is structured as follows: Section 2 briefly summarizes the related literature on the topic. Section 3 presents the different models applied in the empirical analysis, i.e., the dynamic factor model and the four different neural network architectures mentioned above. Section 4 describes the data behind the analysis and exposes the nowcasting exercise. Then, it presents the results of the empirical analysis. Finally, Section 5 concludes.

2 Related works

Giannone et al., 2008 combine a dynamic factor model and the Kalman filter to nowcast the quarterly GDP growth for the US economy. Their two-step approach addresses all three problems of nowcasting mentioned before: it deals with the mixed frequency issue of combining monthly predictor variables and quarterly GDP, it can handle a large number of potential predictor variables, and it can cope with the ragged edge problem of the underlying data. Additionally, it has the potential to capture the essential dynamics of the time series of the panel.

After the seminal work of Giannone et al., 2008, DFMs have been found particularly successful at addressing many of the data issues inherent in nowcasting, and have been applied in many empirical studies (Stock & Watson, 2002). Matheson, 2014 develop monthly indicators for tracking short-run trends in real GDP growth and conduct nowcasting analysis for 32 advanced and emerging-market economies. Marcellino and Schumacher, 2010 conducts nowcasting analysis for the German economic activity, while Chernis and Sekkel, 2017 perform a similar analysis for the Canadian GDP growth.

The fundamental idea of DFMs is that one or more latent factors dictates the movement of many different variables, each with an idiosyncratic component in relation to the factor(s). With historical data, the factor(s) can be estimated from the variables. Subsequently, even in future periods where not all data are complete, the factor(s) can still be estimated and used to generate forecasts for variables that are not yet published, as each variable's relation to the factor(s) has already been estimated. The theory behind the two-step estimator is derived in Doz et al., 2011.

Artificial neural networks (ANNs) have been the catalyst to numerous advances in a variety of fields and disciplines in recent years. Their impact on economics, however, has been comparatively muted. While only a few study of nowcasting has applied ANNs, several other studies have applied neural networks to forecast macroeconomic and financial variables. For example, Tkacz, 2001 uses neural networks to forecast the Canadian GDP growth rate between 1989 and 1992 by applying lagged GDP growth and several other financial variables, such as yield spreads and monetary aggregates. While Tkacz, 2001 uses quarterly data to forecast Canadian GDP by using ANNs, Heravi et al., 2004 apply ANNs to forecast monthly industrial production between 1978 and 1995 for the three largest European economies, with data provided by Eurostat. In contrast to Tkacz, 2001, they only use the information contained in the lagged values of monthly year-on-year growth of industrial production.

Besides these studies, ANNs have also been used in financial forecasting. For instance, Kuan

and Liu, 1995 investigate the forecasting ability of ANNs and recurrent ANNs for daily exchange rates of five major currencies between 1980 and 1985. More recently, Torres and Qiu, 2018 apply recurrent neural networks to daily data of several crypto-currencies, exchange rates, commodities and stocks between 2013 and 2017.

Results of Loermann and Maas, 2019 indicate that the MLP outperforms the dynamic factor model in terms of now- and forecasting accuracy, while it generates at least as good now- and forecasts as the Survey of Professional Forecasters.

Compared to Loermann and Maas, 2019, Hopp, 2021 investigates a more complex recurrent network architecture, namely the long short-term memory network. The paper shows that LSTM networks produce more accurate nowcasts compared with DFMs on three different target series: global merchandise export values and volumes, and global services exports. In addition to better empirical performance for the three target series, LSTMs provide advantages over DFMs by being able to handle large numbers of features without computational bottlenecks and the ability to use any mixture of frequencies in features or target. Disadvantages include the stochastic nature of the parameter estimation and the lack of interpretability in their coefficients (Hopp, 2021). These advantages and disadvantages emerge at a more general level as well, in the comparison of the traditional time series approaches and the artificial neural networks (Goodfellow et al., 2016).

3 Models and methods

3.1 Dynamic factor model

The dynamic factor model (hereinafter, DFM) is a state space model whose main characteristic is that the observation vector is much larger in dimension than the vector of the unobserved (latent) common factors. The general specification of the DFM can be written as follows:

$$\begin{aligned}
 y_t &= \Lambda f_t + Bx_t + u_t \\
 f_t &= A_1 f_{t-1} + \dots + A_p f_{t-p} + \eta_t & \eta_t &\sim N(0, I) \\
 u_t &= C_1 u_{t-1} + \dots + C_q u_{t-q} + \varepsilon_t & \varepsilon_t &\sim N(0, \Sigma)
 \end{aligned}$$

where y_t are observed data, f_t are the unobserved factors (evolving as a vector autoregression), x_t are (optional) exogenous variables, and u_t is the error, or "idiosyncratic" process (u_t is also optionally allowed to be autocorrelated). The Λ matrix is also referred here to as the matrix of *factor loadings*. The variance of the factor error term is set to the identity matrix to ensure identification of the unobserved factors. The size of the observation vector is typically large while the dimension of the state vector is small so we have $p \gg m$ (Durbin & Koopman, 2012).

This model can be cast into state space form, and the unobserved factor estimated via the Kalman filter. The likelihood can be evaluated as a byproduct of the filtering recursions, and maximum likelihood estimation used to estimate the parameters. The (log)likelihood function of the unknown parameters can be formulated as follows (Harvey, 1990):

$$\log L(Y_n) = -\frac{np}{2} \log 2\pi - \frac{1}{2} \sum_{t=1}^n \log |\mathbf{F}_t| - \frac{1}{2} \sum_{t=1}^n \nu_t' \mathbf{F}_t^{-1} \nu_t \quad (1)$$

where p denotes the dimension of the observation vector y_t . The quantities ν_t and F_t are calculated routinely by the Kalman filter, thus $\log L(Y_n)$ is easily computed from the Kalman filter output. We assume that F_t is non-singular for $t = 1, \dots, n$. If this condition is not satisfied initially it is usually possible to redefine the model so that it is satisfied. The representation (1) of the log-likelihood was first given by Schweppe, 1965. Harvey, 1990 refers to it as the *prediction error decomposition*.

The dynamic factor model described above has long been considered the state-of-the-art statistical modeling framework for economic nowcasting. This modeling framework compresses information from a large dataset into a few underlying factors, while at the same time applying Kalman-filtering techniques to fill up the missing data of the ragged edge within the dataframe. Although this approach provides a unified framework incorporating dynamic imputation (model-based interpolation) and nowcasting, the central predictor equation remains linear, potentially restricting the model from generalizing to non-linear patterns (Bartholomew et al., 2011).

3.2 Artificial neural networks

Artificial neural networks (hereafter, ANNs) are flexible nonlinear (universal) estimators which represent the set of alternatives to the benchmark factor model examined in this paper. Similarly to most machine learning algorithms, ANNs can be used for classification problems, predictive exercises where the target variable is categorical, and also for regression function estimation. One of the biggest strengths of ANNs is that they can handle the curse of dimensionality in an *automated* way, much more naturally than traditional time series models. The latter set of models require the preparatory use of a dimension reduction method (e.g., PCA) or an unobserved component model for feature extraction, where the number of potential explanatory variables is large. For example, PCA can give us an optimal lower dimensional representation of the data in the sense that it changes the basis to the direction of maximum variance. However, we cannot be sure if there is no more relevant lower-dimensional representation of the features for the prediction of our target variable. Similarly, when we extract common factors from the input data, the procedure should be driven heavily by our a priori knowledge (choice): We should

have a relatively concrete idea about the potentially relevant explanatory variables (features). After the set of observable indicators have been defined, method of explanatory factor analysis extracts common factors in such a way that they can explain the co-movements, i.e., the covariance structure of our features best. Here we see again that feature extraction is somewhat separated from the essential modeling task. Hence, it is not surprising that DFM-based GDP nowcasting is referred to as a two-staged estimation procedure in the literature (Giannone et al., 2008). By contrast, ANNs, can, in principle at least, learn the relevant feature representation by themselves.

The demand to connect the feature extraction with the actual predictive modeling task arises naturally and justifiably. Here is where artificial neural networks perform really well because they are inherently capable of learning the relevant representation of the features for the prediction of the target variable.¹

This is not to say however, that ANNs are generally superior modeling frameworks compared to traditional linear models. While ANNs handle the *curse of dimensionality* more easily, they can perform worse in other areas. For example, they require a much more sophisticated data pre-processing step where we must deal with missing observations as well. One possible solution to fill up missing values is applying univariate ARMA(p,q) forecasts for each single input series. In this case, the lag lengths of the individual ARMA(p,q) models can be selected based on the value of Akaike or Schwarz information criterion (Greene, 2017, Loermann and Maas, 2019). Although missing data issue for ANNs can be solved in many ways, state space models handle this problem by design.

If we think about the three big challenges of nowcasting mentioned in the introduction, we can say that mixed-frequency data can be treated relatively well in both modeling frameworks. Compared with the DFM, proper construction of our training and test samples with mixed-frequency data may require some additional effort.

More generally, we should also mention that even the smallest ANNs have much more parameters than a typical statistical model. The large number of trainable (*free*) parameters results in a relatively large hypothesis space. From the bias-variance trade-off follows that with a larger hypothesis space, it is more likely to find a hypothesis which fits the training data very well. This phenomenon is called overfitting, and it happens when a model learns the fine details and noise in the training data rather than the actual **systematic** relationship between the regressors and the target variable(s). Overfitting can substantially weaken a statistical model's generalization

¹We should note that this kind of *connected* feature extraction (with some limitations) can be conducted with statistical models as well, but traditional statistical models are clearly more limited in this regard.

capability, and ANNs are substantially more prone to overfitting compared to the traditional time series models.

So far, we tried to summarize the most important characteristics of ANNs as one of our nowcasting machines. In the following sections, we investigate those architectures in more detail that were adopted in the empirical analysis.

3.2.1 Multilayer perceptron

While a single Rosenblatt perceptron can be used as a linear classifier, its straightforward extension, the multilayer perceptron (MLP) with non-linear activation functions, can perform non-linear classification and regression tasks as well.² This neural network is one of the simplest examples of a fully connected feedforward network.

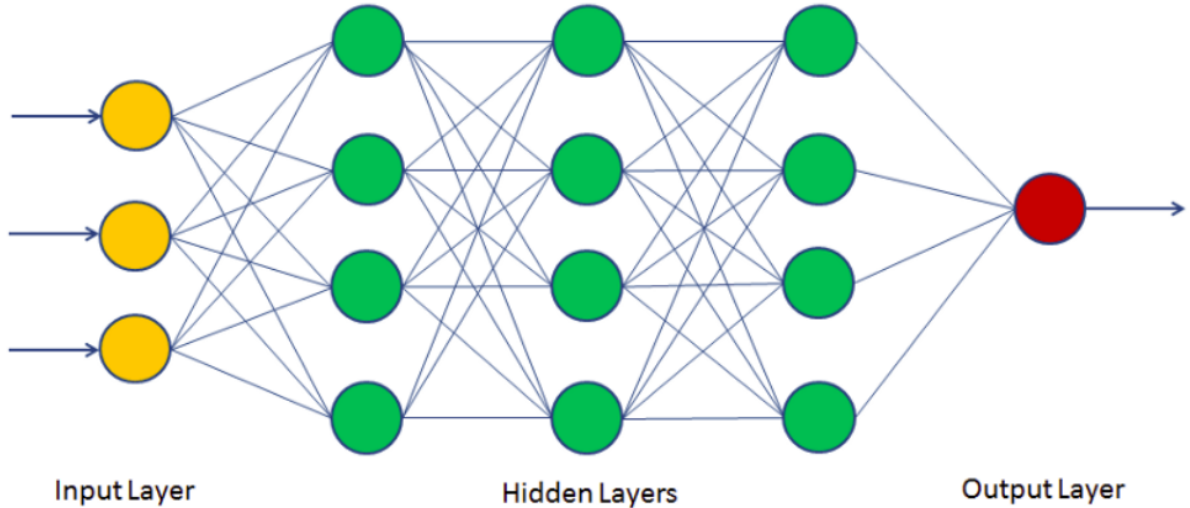


Figure 1: Multilayer perceptron.

According to Figure 1, the MLP’s input-output mapping – if we assume the same non-linearity in each layer – is as follows:

$$\mathbf{y} = f(\mathbf{w}^L f(\mathbf{w}^{L-1} f(\mathbf{w}^{L-2} \dots f(\mathbf{w}^1 \mathbf{x})))) \quad (2)$$

where \mathbf{w}^L is the matrix combining the weight vectors of the neurons in the l -th layer, and $f(\cdot)$ denotes the activation functions (sigmoid) applied to the outputs of the neurons belonging to the same layer. An MLP, even in its simplest form when it contains one hidden layer, implements a non-linear mapping on its parameters. As equation (2) suggests each hidden layer of an MLP

²Hereafter, we refer to a perceptron as a neuron because the perceptron is just a special type of neuron (just like the Adaline for example), and we prefer the more generic name *neuron*.

can learn an arbitrary affine transformations of its inputs.³ As we will see below, this kind of universality will also affect the generalization capability of the network.

While MLPs can be used in time series forecasting, we should see that its architecture lacks any explicit temporal aspect. As long as any hidden layer can learn an arbitrary affine transformation of its inputs, the size of the hypothesis space can be even too large for our purposes. Notwithstanding that MLPs can learn time-invariant mappings between their inputs and outputs, their inner (hidden) structure is not invariant to shifts (translations) in time. A more fitting feedforward architecture for time series prediction can be the time-delay neural network, or in other words, the one-dimensional convolutional neural network (1D CNN).

3.2.2 1D Convolutional network

Convolutional Neural Networks (CNNs), similarly to MLPs, are also feedforward neural networks that consist of convolutional and pooling (subsampling) layers. 2D CNNs have become the standard for various computer vision tasks in the last decade. As the field of application of 2D CNNs has constantly broadened, 1D CNNs have also received growing attention. 1D CNNs have recently been proposed and achieved state-of-the-art performance levels in several applications, such as biomedical data classification, anomaly detection, and structural health monitoring (Kiranyaz et al., 2021). Nevertheless, we have not yet seen any application in the literature which is specifically related to economic nowcasting or forecasting. In the following, we try to argue that this type of empirical exercise possesses characteristics that render the application of 1D CNNs a suitable choice.

First, we want to find a time-invariant mapping between our features and our target variable. Intuitively, this means that the same feature vector should have the same response in the target variable, even if it is shifted in time – assuming steady state. While MLPs can also learn time-invariant mappings, their intrinsic architecture, which favors flexibility, does not enforce this type of restricted learning. Since 1D CNNs, in their convolutional layers, learn the coefficients of multiple finite impulse response filters, they can only learn time-invariant mappings by definition. In other words, the network’s architecture intrinsically restricts the hypothesis space to the composition of time-invariant mappings, which we supposedly want to find in the nowcasting analysis of a stationary time series. Figure 2 below shows a simple example of single channel 1D convolution, where the input sequence size is 7 and the filter (kernel) size is 3.

³An affine transformation is the combination of linear transformation with translations. Translation can be learned through the bias.)

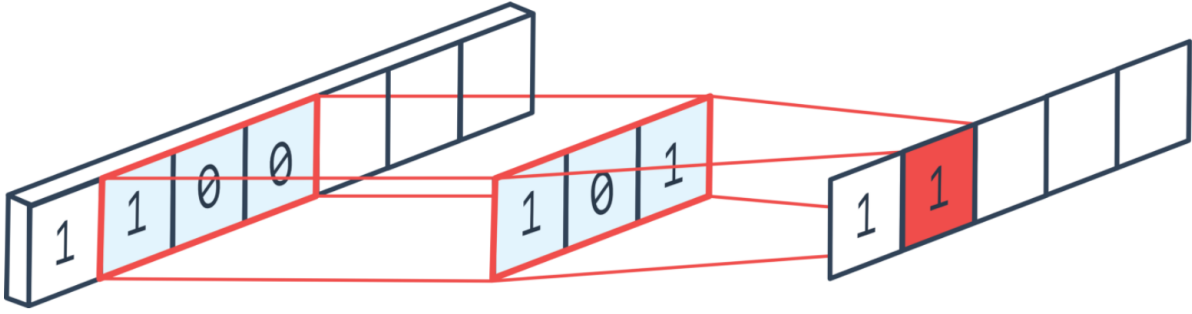


Figure 2: Single channel 1D convolution. Source: Ganesh, 2019.

Figure 2, shows that a 1D CNN practically realizes finite impulse response filters on its inputs, where filter coefficients are estimated during the training process. Based on this simple example, we can also see that unlike MLPs, 1D CNNs are trained with sequential data where the network receives a fixed size input sequence in each t time step. Obviously, in more complex cases we can have multiple input series (features) and multiple output channels as well.

Figure 3 below illustrates a case where we have 4 input features (i.e., the input depth is 4), a filter the size (length) of which is 5, and 4 output channels (i.e., the output depth is 4). As Figure 3 suggests, in a convolutional layer, we will have a separate filter corresponding to each channel of the feature map.

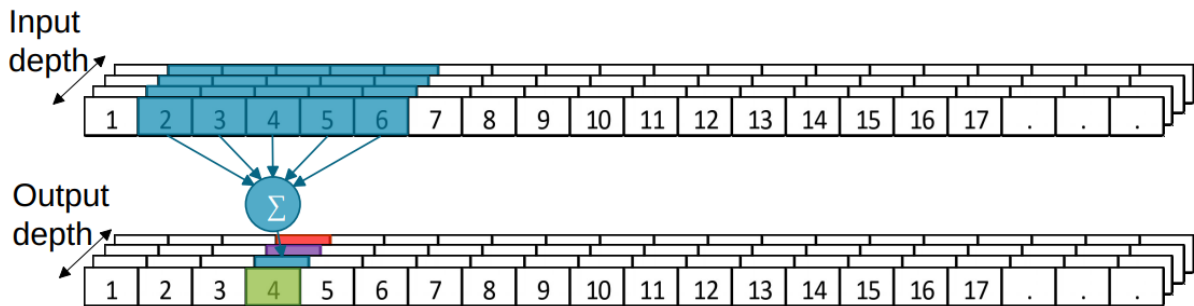


Figure 3: 1D convolution with multiple input features and output channels.

Summarizing the above, the inclusion of 1D CNN layers enables the network to learn its own internal representation of sequential (time series) data. Hence, 1D CNNs are trained with sequences where time series data are split into fixed-sized windows (sequences). Since their architecture represents a feedforward network, similar to the MLP, only the data points inside that window (input sequence related to time t) can affect the outcome at time t . Recurrent neural networks (hereafter, RNNs) remove this key restriction by allowing loops in their computational graph. Through this feedback loop, RNNs can remember data points much further in the past than a typical window size.

3.2.3 Gated recurrent networks

As opposed to the unidirectional relationship between inputs and outputs, previously seen in feedforward networks, RNNs introduce a feedback loop, where layer outputs can be fed back into the network (Dematos et al., 1996). This architecture makes RNNs well-suited to applications with a temporal aspect or flow, such as natural language processing or speech processing.

A recurrent neural network (RNN) is a class of artificial neural networks where connections between nodes can create a cycle, allowing output from some nodes to affect subsequent input to the same nodes. This allows it to exhibit temporal dynamic behavior. Derived from feedforward neural networks, RNNs can use their internal state (memory) to process variable length sequences of inputs. This makes them applicable to tasks such as unsegmented, connected handwriting recognition, speech recognition or time series analysis. However, due to vanishing gradients, RNNs tend to have a very "short,, memory, limiting their usefulness in the nowcasting application (Ekman, 2021).

In our paper, we do not investigate RNNs in general but focus on their more advanced variants that implement a so-called gating mechanism, namely the long short-term memory network (LSTM) and the gated recurrent unit (Hochreiter and Schmidhuber, 1997, Chung et al., 2014).

Long short-term memory (LSTM) network is a special form of gated RNNs which was introduced by Hochreiter and Schmidhuber, 1997. A common way of drawing LSTM was introduced in a popular blog post that explains how LSTM works (Olah, 2015). Our summary on LSTMs is based on Ekman, 2021, Goodfellow et al., 2016 and Olah, 2015.

Figure 4 below, illustrates an LSTM layer unrolled in time for three timesteps. For each timestep t , the corresponding cell receives c_{t-1} and h_{t-1} from the previous timestep (cell) and x_t from the current timestep and outputs new values for the cell state (c) and the hidden state (h). Accordingly, h_t and c_t denote the *hidden state* (also referred to as the *output* of the LSTM cell) and the *cell state* (also known as the *internal state*) at time step t , respectively.

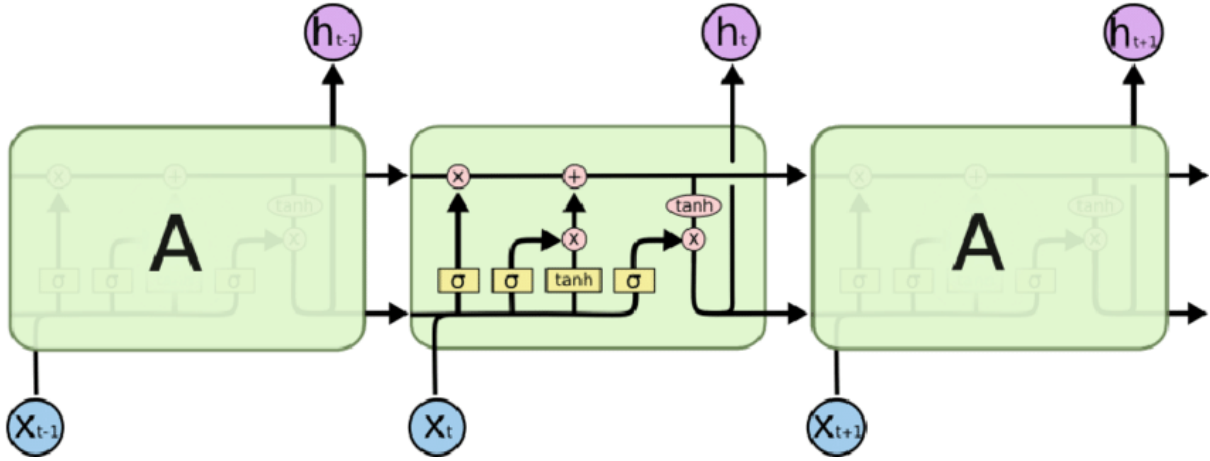


Figure 4: LSTM layer unrolled in time. Source: Olah, 2015

As Figure 4 illustrates, LSTM introduces a memory cell and three gates: an input gate, an output, and a forget gate. Essentially, the architecture then allows gradients to flow unchanged through the so-called *gradient highway*, mitigating the vanishing gradient problem of standard RNNs and rendering them more suitable for applications where long memory matters. Considering our empirical analysis, we are interested to see whether allowing for long memory does lead to better nowcasts.

Gated recurrent unit (hereafter, GRU) represents the other gated recurrent network adopted in our nowcasting analysis. Considering its architecture, GRU is very similar to an LSTM but belongs to a newer generation of gated RNNs (Chung et al., 2014). The GRU removes the cell state (denoted by c_t in the LSTM) and uses its hidden state (denoted by h_t , similar to the LSTM) even for transferring information. This way, it only has two gates, a reset gate and an update gate.

Thereby, GRUs has fewer parameters and tensor operations compared to LSTMs (Chung et al., 2014). Consequently, they are a little speedier to train, and a bit less prone to overfitting. Researchers and engineers usually try both to determine which one works better for their use case. So we do the same in empirical analysis. Similarly to 1D CNNs, both LSTMs and GRUs are trained with sequential data.

We have seen that gated RNNs provide a solution to the vanishing gradient problem through different gating mechanisms. This way, they can explore long-term dependencies in the sequences and connect information from the past to the present. Considering our empirical analysis, it is an essential question if there are such input sequences whose much older values have a significant impact on current-quarter GDP growth while that impact is no longer reflected in any more recent values of the sequences. To put this question into a more formal manner, let us consider

the conditional probability distribution of our target variable. If we assume that GDP growth has no long-term memory, i.e., that it is ergodic, then the following equation is expected to hold for a given sequence length (l) and for all $t^* < t - l$ time period – at least, approximately:

$$\mathbb{P}(y_t|\Omega_{t^*}, \Omega_t) = \mathbb{P}(y_t|\Omega_t), \quad (3)$$

where $\mathbb{P}(y_t|\Omega_{t-1})$ denotes the conditional probability distribution of y_t conditional on the information set $\Omega_t = [\mathbf{x}_t, y_{t-1}, \mathbf{x}_{t-1}, \dots, y_{t-l+1}, \mathbf{x}_{t-l+1}]$. This question is of essential relevance to our analysis because the choice of the fitting neural network architecture largely depends on what we think about the data-generating process of GDP growth. In other words, in the context of system theory, what do we think about the impulse response function of the target variable? It is worth noting that both the MLP and the 1D CNN build around the assumption of fixed finite support for their target variable, in our case, GDP growth.⁴ While gated RNNs still assume a finite impulse response for the target variable, they allow for a much longer support. Furthermore, through their gating mechanism, they can dynamically adjust for the length of the impulse response. With this type of flexibility, however, comes complexity (much more trainable parameters) as well.

We should also note that gated RNNs are even more complex than those standard RNNs: While in standard RNNs cells are represented by a single neuron, LSTM and GRU cells contain several neurons inside, requiring at least a matrix for every gate. As a result, they are more prone to overfitting and highly sensitive to input noise. Moreover, due to their feedback loop, the stability analysis of (gated) RNNs is also more complicated than the feedforward networks. Even the initialization of such recurrent networks can be complicated in many cases (Ekman, 2021). On the other hand, if we think about the economy as a system with a long memory, then gated RNNs might provide more accurate nowcasts than any previously presented architectures, despite the aforementioned difficulties.

Below, in the empirical analysis, we let the data speak and evaluate the results of different models. In addition to the DFM, the state-of-the-art representative of traditional time-series approaches, we apply four different network architectures from the ANNs' side. We believe that this type of an analysis might be informative about the competitor models' nowcasting performance and some important aspects of GDP growth as well.

⁴The support of a real-valued function $f(\cdot)$ is the subset of the function domain containing the elements which are not mapped to zero. In our case, finite support means that the impulse response is bounded in time.

4 Empirical analysis

In this section, we first describe the data used in the empirical analysis then define the concrete nowcasting exercise. After that, we present the results of the empirical analysis.

4.1 Description of data

The target variable of the empirical analysis is the quarterly GDP growth, that is the percent change (relative to the preceding period) of the US Gross Domestic Product. The series is measured on a quarterly frequency and is available from 1947:Q2 to 2022:Q3. Thus it contains 302 observations. Figure 5 plots the time series for quarterly GDP growth.



Figure 5: The percent change (relative to the preceding period) of the US Gross Domestic Product. Source: FRED-MD.

When the empirical analysis was closed, the last GDP measurement was released for 2022:Q3. This release was revised later, in December. So the fundamental idea of nowcasting, using the informational content of higher-frequency data to help the prediction of our target variable, seems valid in this case. In our empirical analysis, we try to extract the informational content of several monthly macroeconomic indicators (i.e., features) whose intra-quarterly development might be expressive of the current economic growth.

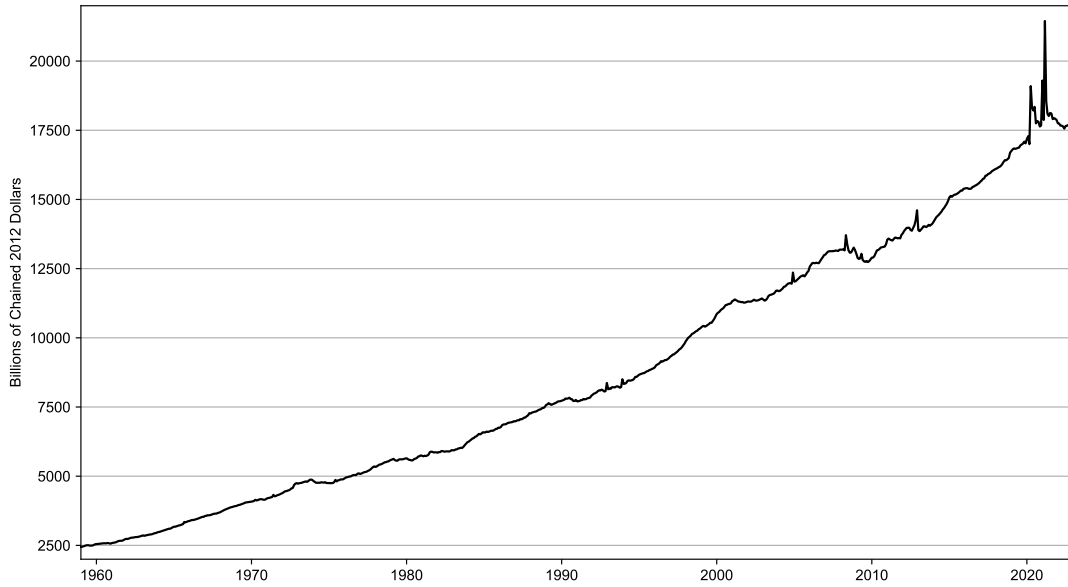
The data for the input features comes from the FRED-MD database, the monthly database for Macroeconomic Research of the Federal Reserve Bank of St. Louis, which is described

extensively in McCracken and Ng, 2016. FRED-MD is a large macroeconomic database that is designed for the empirical analysis of “big data”. The database is publicly available and updated in real-time on a monthly basis. The FRED-MD database is available for download under the following link: <https://research.stlouisfed.org/econ/mccracken/fred-databases/>. It consists of 134 monthly time series (indicators or features) which are clustered into eight categories:

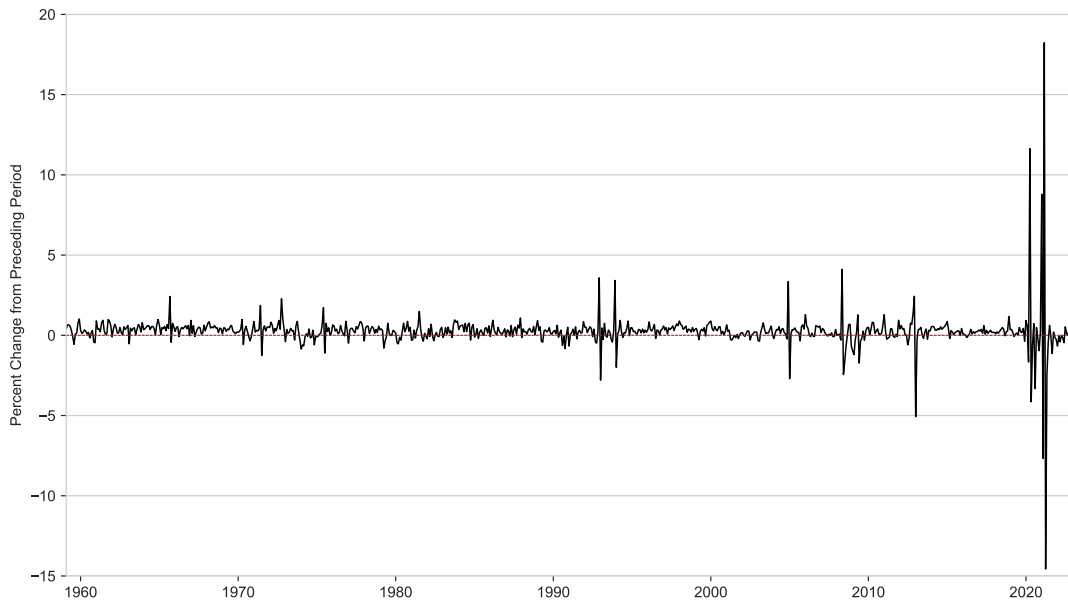
1. Output and income (17 series)
2. Labour market (32 series)
3. Housing (10 series)
4. Consumption, orders and inventories (14 series)
5. Money and credit (14 series)
6. Interest and exchange rates (22 series)
7. Prices (21 series)
8. Stock market (4 series)

The complete list of the data and the series-related data transformations are described in detail in Appendix A.1. Monthly indicator data are available from 1960:M1 to 2022:M9, so we have 753 observations for the potential regressors.

It is important to note that as a result of the corresponding data transformation, all of the monthly indicators (features) are transformed into stationarity. Except for the MLP, all of our models are designed to estimate time-invariant prediction rules, which is preferred for stationary time series. In this case, where both the target variable and the regressors (features) are stationary, we can generally expect better predictive performance from these models compared to when modelling non-stationary series. Figure 6 below shows the level values of Real personal income (upper panel) and the result of the adequate stationarity transformation (lower panel).



(a) RPI: Original, non-stationary time series



(b) RPI: Log-differenced, stationary time series

Figure 6: Real personal income (RPI). Source: FRED-MD.

For the training of the different ANNs, we use the same sixteen selected indicator series from the FRED-MD database.⁵ To estimate the DFM, we use an even more restricted subset of the monthly indicators. Unlike the different ANN architectures presented in our study, the DFM's computation time scales exponentially with the number of input features (i.e., regressors (Hopp, 2021)). In the case of the DFM, feature selection is also separated from the actual predictive step.

⁵We are currently working on an automated systematic feature selection procedure, the results of which might be presented in the next version of this paper.

These two idiosyncrasies can make the process of feature selection a much more complicated task than that is usually experienced with different ANNs. Based on these considerations, we used the following four monthly macro indicators during the course of the DFM-based nowcasting routine.

- Industrial production: Manufacturing (IPMANSICS)
- Real aggregate income (excluding transfer payments) (W875RX1)
- Manufacturing and trade sales (CMRMTSPL)
- Employees on non-farm payrolls (PAYEMS)

These series are proposed by the related documentation of the *statsmodels* Python module (Seabold & Perktold, 2010). All of these series are also included in the FRED-MD dataset.

4.2 Exposition of the nowcasting exercise

Our full dataset ranges from 1960:Q1 to 2022:Q3, so that it contains feature observations for every month and target observations for every third month (i.e., for every quarter). We assume that quarterly measured GDP observations are available for months M3, M6, M9, and M12.⁶ Our training dataset ranges from 1960:Q1 to 2009:Q4. Thus it contains 200 observations for quarterly GDP growth and 600 observations for the monthly indicators (features). We evaluate the results from two test (evaluation) periods in the empirical analysis. The first evaluation period ranges from 2010:Q1 to 2019:Q4, so it ends before the COVID-19 pandemic hits the US economy. It includes 40 observations for the target variable and 120 measurements for the monthly indicators. In comparison, the second evaluation period lasts until 2022:Q3, so it also includes those periods of the COVID crisis. Specifically, it ranges from 2010:Q1 to 2022:Q3, containing 51 target and 153 feature observations. Consequently, we can see the results from two distinctly different evaluation periods. The first is mainly characterized by the balanced economic growth after the Great Recession, while the second is heavily affected by the economic impacts of the COVID-19 pandemic.

In addition to the two separate evaluation periods, we evaluate the results of three different nowcasting scenarios, depending on the information set available for our models. The *1-month* nowcasting scenario presumes that the monthly indicators' value is available up through the

⁶FRED data releases associate these quarterly measurements with timestamps M1, M4, M7, and M10. However, using these timestamps would be highly counter-intuitive in this type of analysis. Following the literature, we assume that quarterly GDP measurements are published at the end of the current quarter. In reality, the first measurements are usually available only a few months after the end of the current quarter.

first month within a quarter. In the *2-month* scenario, the information set also contains feature observations released until the second month within the current quarter. Finally, in the *3-month* scenario, we use all monthly indicator data available at the end of the current quarter. If we define the nowcast as the conditional expected value of current-quarter GDP growth (y_q), we can write as follows (Giannone et al., 2008):

$$\hat{y}_q = \mathbb{E}(y_q | \Omega_v, \mathcal{M}), \quad (4)$$

where $t = 1, 2, \dots$ denotes months, $q = 3t$ denotes quarters, Ω_v represents the information set containing monthly indicator data until the v -th month and $v = [3t - 2, 3t - 1, 3t]$. Lastly, \mathcal{M} represents the underlying model. Based on 4, we see that different nowcasting scenarios mentioned above only differ in their corresponding information set. More specifically, $v = 3t - 1$ refers to the 2-month nowcasting scenario. So within a given quarter, training sequences of length l include observations for monthly indicators until the second month. Intuitively, we expect to see the most accurate nowcasts in the 3-month nowcasting scenario ($v = 3t$), where all intra-quarterly indicator data are available for prediction. In equation 4, \mathcal{M} denotes a concrete element of the set of our (competitor) models (DFM, MLP, 1D CNN, LSTM, GRU). The underlying model determines what function $f(\cdot)$ can be learned between the target variable and the regressors during the training (estimation) process. In the line of the above, the nowcast for quarter q can be generated as follows:

$$\hat{y}_q = f(\mathbf{x}_v, \mathbf{x}_{v-1}, \dots, \mathbf{x}_{v-l+1}) \quad (5)$$

where \mathbf{x}_v represents a row in the regressor vector, containing observations for n number of features in month v . As equation (5) suggests, we do not include any lagged values of the target variable in the regressor vector, which is denoted by $\varphi(\mathbf{x}_v)$. Hence, if l denotes the length of the training sequences (i.e. sequences of monthly indicators), the dimensionality of the regressor vector is $l \times n$. Training samples $(\varphi(\mathbf{x}_v), y_q)$ are formed then by pairing the actual target observations for quarter q with the corresponding regressor vector. For training samples, $q \in \{1960 : Q1, \dots, 2009 : Q4\}$.

All of our models are estimated (trained) on a fixed-size, static training window, which ranges from 1960:Q1 to 2019:Q4. So it contains 200 observations for quarterly GDP growth. Accordingly, the training dataset has 600 measurements for the monthly indicators (regressors). Training sequences are sampled then by a fixed-length rolling window where the size of the rolling window is determined by the sequence length (l). Since each (sub)sample of the features is related to a given quarterly target observation, successive rolling windows differ in values for their last 3 months. Consequently, they overlap in $l - 3$ monthly values, provided that $l > 3$.

As a criterion (loss) function, we apply the mean squared error according to equation 4. Our training setup ensures that the weights, estimated values of the trainable parameters, are the same for both evaluation periods. Based on (5), we generate the series of nowcasts for the first evaluation period where $q \in \{2010 : Q1, \dots, 2019 : Q4\}$. We do the same for the second test period, where $q \in \{2010 : Q1, \dots, 2022 : Q3\}$.

The predictive accuracy of the competitor models is evaluated relative to the so-called naive constant growth model. The naive growth model is a basic benchmark model that assumes constant growth for GDP. From a computational point of view, this means that the nowcast for quarter q is assumed to be equal to its previous actual value: $\hat{y}_q = y_{q-1}$. While even this simple approach might have some theoretical background, its predictive performance is expected to be weak, especially in periods of high economic turbulence. Figure 7 below, illustrates the predictive performance of the naive constant growth model during the two evaluation periods.

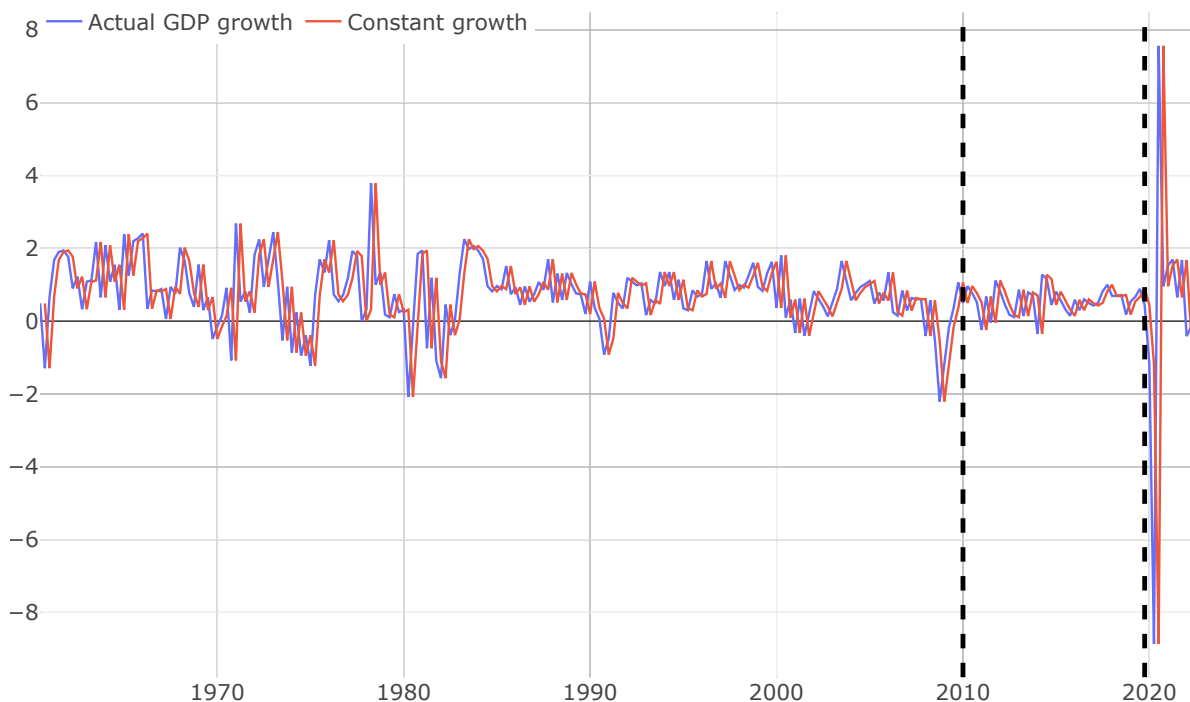


Figure 7: Nowcasting performance of the naive constant growth model. The first evaluation period ranges from 2010:Q1 to 2019:Q4. The second evaluation period is from 2010:Q1 to 2022:Q3. Source: Own editing based on the FRED-MD database.

In Figure 7, we see that the naive growth model fits the data relatively well in normal economic circumstances (e.g., during the first evaluation period). It clearly fails however when large shocks (positive or negative) hit the economy, just like during our test period. The economic impact of the COVID-19 pandemic resulted in a V-shaped recession: a sharp downturn in 2020:Q2

followed by a quick rebound in growth in 2020:Q3. While signs of the economic downturn had been clearly visible by April or May, the naive benchmark model totally misses to predict the forthcoming recession. We believe that it is an interesting question in itself, how accurately our competitor models can predict this sharp V-shaped recovery? We evaluate the nowcasting accuracy of our models in terms of root mean squared error (RMSE) and mean absolute error (MAE). As a benchmark, the constant growth model generates an RMSE value of 0.538 and an MAE value of 0.414 during the first test period. These measures for the second test period are 2.781 and 1.078, respectively. These values provide the basis for model evaluation and also help to indicate the competitor models' absolute nowcasting accuracy.

4.3 Results

In the following, we present the results of the empirical analysis. As the COVID-19 pandemic hit the US economy in 2020, we decided to evaluate our models on two different evaluation periods: The first evaluation period ranges from 2010:Q1 to 2019:Q4, so it does not reflect the economic impact of the COVID-19 pandemic. In comparison, the second evaluation period is from 2010:Q1 to 2022:Q3, containing those periods of the COVID crisis as well. We believe that the results from these two evaluation periods show a more balanced and well-rounded picture of the different models' nowcasting performance. Clearly, these two test periods are very different in their characteristics. The first can be basically described as a period of balanced economic growth. Under such circumstances, the naive benchmark model is expected to be a strong contender for our competitor models. Consequently, competitor models should accurately predict even more intricate movements in economic growth to beat the benchmark model. In contrast, the second evaluation period would favor the models that can capture the sharp V-shaped recovery of 2020:Q2 and 2020:Q3. We believe that results from these two evaluation periods will provide a robust assessment about the generalization capability of the different competitor models, showing their strengths and weaknesses.

Below, Table 1 presents the results of the nowcasting competition in our first evaluation (test) period, which ranges from 2010:Q1 to 2019:Q4. Table 1 also shows how the length of the training sequences affect the competitor models' nowcasting accuracy: For the MLP, we formed input sequences of four different lengths by hand: $l = [4, 8, 18, 36]$. Similarly, we investigated three different sequence length configurations for the other ANN architectures to be trained with input sequences: $l = [8, 18, 36]$. In the line of the above, n refers to the number of features (regressors) selected for training (estimation).

Table 1: Nowcasting performance of the competitor models relative to a naive constant growth model for GDP: RMSE and MAE evaluation. Evaluation period: 2010:Q1 – 2019:Q4.

	$v = 3t - 2$		$v = 3t - 1$		$v = 3t$	
	RMSE	MAE	RMSE	MAE	RMSE	MAE
DFM (n=4)	0.755*	0.777*	0.706**	0.725**	0.712**	0.719**
MLP (n=16, l=4)	1.146	1.049	0.924	0.846	0.935	0.886
MLP (n=16, l=8)	1.048	0.981	0.906	0.996	1.008	1.045
MLP (n=16, l=18)	0.851	0.931	0.752**	0.759**	0.833*	0.853
MLP (n=16, l=36)	0.938	0.942	1.090	1.154	0.923	1.018
1D CNN (n=16, l=8)	1.053	1.086	0.948	0.981	0.677**	0.715**
1D CNN (n=16, l=18)	0.892	0.919	0.943	0.939	0.748**	0.769**
1D CNN (n=16, l=36)	0.952	0.981	1.056	1.127	0.816	0.874
LSTM (n=16, l=8)	0.759*	0.743*	0.915	1.002	0.775*	0.769**
LSTM (n=16, l=18)	0.673**	0.699**	0.869	0.965	0.673**	0.677***
LSTM (n=16, l=36)	0.621**	0.644***	0.945	1.056	0.776*	0.782*
GRU (n=16, l=8)	0.659**	0.684**	0.903	0.905	0.605***	0.592***
GRU (n=16, l=18)	0.646**	0.682**	0.829	0.843	0.632***	0.631***
GRU (n=16, l=36)	0.643**	0.652***	0.811	0.781	0.674**	0.675**

Notes: This table reports the relative RMSE and MAE of GDP growth for our competitor models relative to a naive constant growth model for GDP. A value below one indicates that the competitor model beats the naive benchmark model. The stars denote statistical significance at 10%(*), 5%(**) and 1%(***) level of the one-sided Diebold and Mariano, 1995 test. Columns are related to the individual nowcasting scenarios: e.g. $v = 3t - 2$ refers to the 1-month nowcasting scenario.

First, it is apparent that all of the competitor models can outperform significantly the naive benchmark model, at least under some configurations. Given that the entire sample period was characterized by balanced and stable economic growth, the results of Table 1 seem to justify the use of this type of modeling exercise. In accordance with the recent literature, we see that application of neural networks for economic nowcasting can yield significantly more accurate nowcasts than the naive growth model. Results of Table 1 also suggest that some ANN

architectures can beat even the DFM in terms of nowcasting performance: While the DFM can beat the naive benchmark model only on a 5% significance level, the LSTM and the GRU beat it on a 1% level under different configurations. Focusing on the nowcasting performance of the different ANNs, the lack of any temporal aspect clearly hinders the MLP during the test period. As Table 8 shows, it can only outperform the naive benchmark model under just one configuration ($n = 16, l = 18$). Compared to the MLP, 1D CNN generates considerably better nowcasts in the first evaluation period. When indicator data is available until the last month within a quarter, 1D CNN beats the naive benchmark model on a 5% significance level. Clearly though, gated RNNs produce even more accurate nowcasts, according to both evaluation metrics as they beat the constant growth model on a 1%. The overall best-performing model is the GRU which produces a 0.605 relative RMSE and a value of 0.592 of MAE, beating the benchmark model on a 1% significance level.

It is interesting to see that the increase of the sequence length above a given threshold does not improve the nowcasting performance of the competitor models. Moreover, this particular threshold for sequence length also seems to be quite stable between the different network architectures. LSTM is the only exception where the increase of the sequence length from 18 to 36 resulted in more accurate results in the 1-month nowcasting scenario. However, longer sequences did not generally yield better nowcasts, even for the LSTM, because the configuration with input sequences of length 18 proved to be an equally good choice. Considering the nowcasting accuracy of the GRU, it is safe to say that the increase of the sequence length does not improve the nowcasting performance. In fact, the configuration with the shortest input sequences generated the most accurate results in our first evaluation period. Figure 8 plots the nowcasts generated by the best GRU configuration and the actual values of GDP growth.

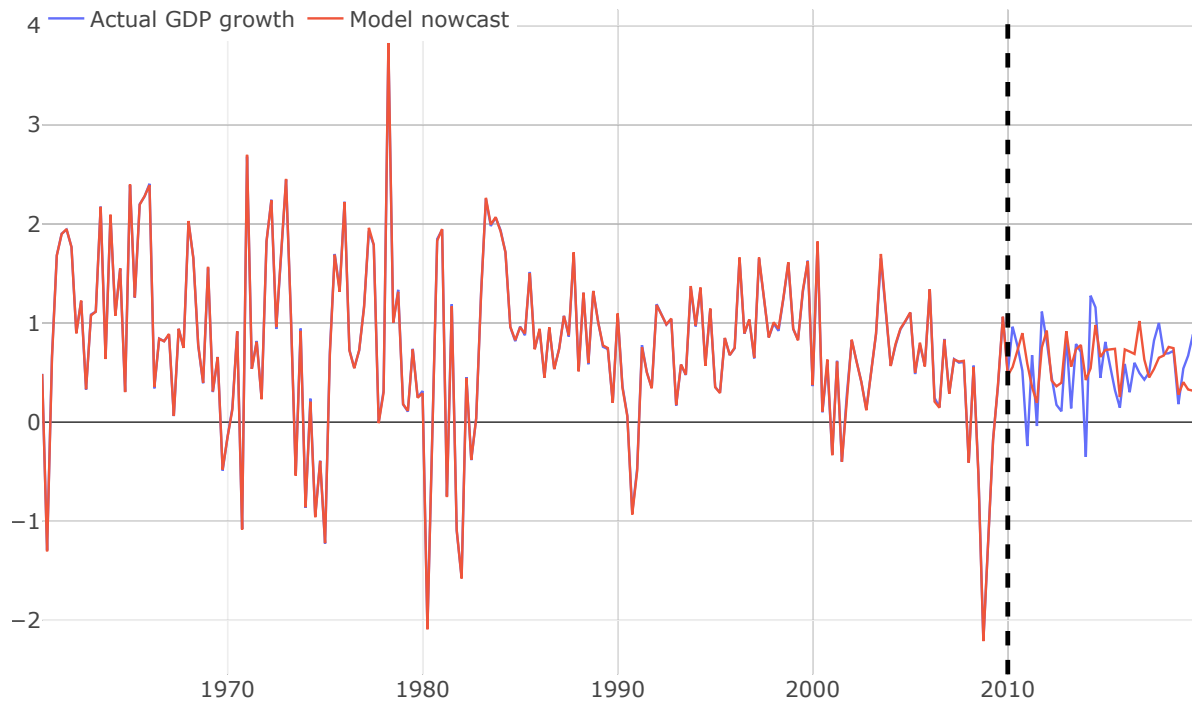


Figure 8: Nowcasting performance of the GRU ($n=16$, $l=8$). Evaluation period ranges from 2010:Q1 to 2019:Q4. Source: Own editing based on the FRED-MD database.

After we have seen the results for our first test period, Table 2 presents the outcome of the nowcasting competition for our second evaluation period which ranges from 2010:Q1 to 2022:Q3.

Table 2: Nowcasting performance of the competitor models relative to a naive constant growth model for GDP: RMSE and MAE evaluation. Evaluation period: 2010:Q1 – 2022:Q3.

	$v = 3t - 2$		$v = 3t - 1$		$v = 3t$	
	RMSE	MAE	RMSE	MAE	RMSE	MAE
DFM (n=4)	0.615	0.707	0.519	0.628*	0.525	0.618*
MLP (n=16, l=4)	0.436	0.577*	0.234*	0.426**	0.219*	0.400**
MLP (n=16, l=8)	0.344	0.550*	0.234*	0.479**	0.217*	0.442**
MLP (n=16, l=18)	0.303*	0.554*	0.391	0.594*	0.432	0.666*
MLP (n=16, l=36)	0.418	0.582*	0.471	0.656*	0.475	0.652*
1D CNN (n=16, l=8)	0.293*	0.581*	0.294*	0.530*	0.297*	0.472**
1D CNN (n=16, l=18)	0.562	0.678	0.532	0.715	0.494	0.647
1D CNN (n=16, l=36)	0.296*	0.526*	0.647	1.072	0.563	0.690*
LSTM (n=16, l=8)	0.473	0.559**	0.546	0.673	0.542	0.628*
LSTM (n=16, l=18)	0.463	0.578**	0.558	0.701	0.512	0.579**
LSTM (n=16, l=36)	0.424	0.497**	0.561	0.707	0.538	0.608*
GRU (n=16, l=8)	0.426	0.532**	0.547	0.641*	0.506	0.527**
GRU (n=16, l=18)	0.380*	0.514**	0.520	0.609*	0.518	0.547**
GRU (n=16, l=36)	0.402*	0.506**	0.541	0.605*	0.492	0.546**

Notes: This table reports the relative RMSE and MAE of GDP growth for our competitor models relative to a naive constant growth model for GDP. A value below one indicates that the competitor model beats the naive benchmark model. The stars denote statistical significance at 10%(*), 5%(**) and 1%(***) level of the one-sided Diebold and Mariano, 1995 test. Columns are related to the individual nowcasting scenarios: e.g. $v = 3t - 2$ refers to the 1-month nowcasting scenario.

Table 2 shows that all the competitor models have a better relative nowcasting performance than in the first evaluation period. Controversially, in terms of statistical significance, we see quite the opposite picture: None of the competitor models can beat the naive benchmark model on a 1% significance level, which applies to our evaluation metrics. The reason for this counter-intuitive phenomenon can be traced back to the special characteristics of the evaluation period. The sharp V-shaped recession in 2022:Q2 and Q3 is indicated by extreme values (*outliers*) in

the target series. In these periods, the naive benchmark model, which assumes constant growth, performs particularly poorly. Recalling the formula of the Diabold - Mariano test statistic, these extreme values affect the variance of the loss differential (series) much more than its mean. In the following version of this paper, we plan to adopt an evaluation method more suitable to the characteristics of the second test period.

Nonetheless, the results of Table 2 provide some valuable insights into the generalization capabilities of the different models and the role of long-term memory. Here, the MLP’s simple yet highly flexible architecture results in highly accurate nowcasts. Concretely, best MLP configurations consistently beat the benchmark model on a 5% significance level in terms of MAE evaluation and on a 10% significance level in terms of RMSE. It is apparent that the best-performing configurations are the ones trained with shorter input sequences ($l = 4, 8$). These configurations detect the COVID-crisis particularly well which leads to remarkably good relative performance in term of RMSE.

Considering the other time-invariant architectures, 1D CNN is the only one which comes close to MLP’s performance. Some 1D CNN configurations with shorter sequences can detect the COVID crisis almost as good as the best MLPs. The configuration with 8 long input sequences actually beats the benchmark model in all the nowcasting scenarios. The relatively weak performance of the gated RNNs suggests that long-term memory does not help predict sharp changes in economic growth, just like the V-shaped recession of 2020:Q2 and Q3. Architectural constraints providing time-invariant behavior also seem more of a handicap as well.

Figure 9 plots the nowcasts generated by our best MLP configuration and the actual values of GDP growth.

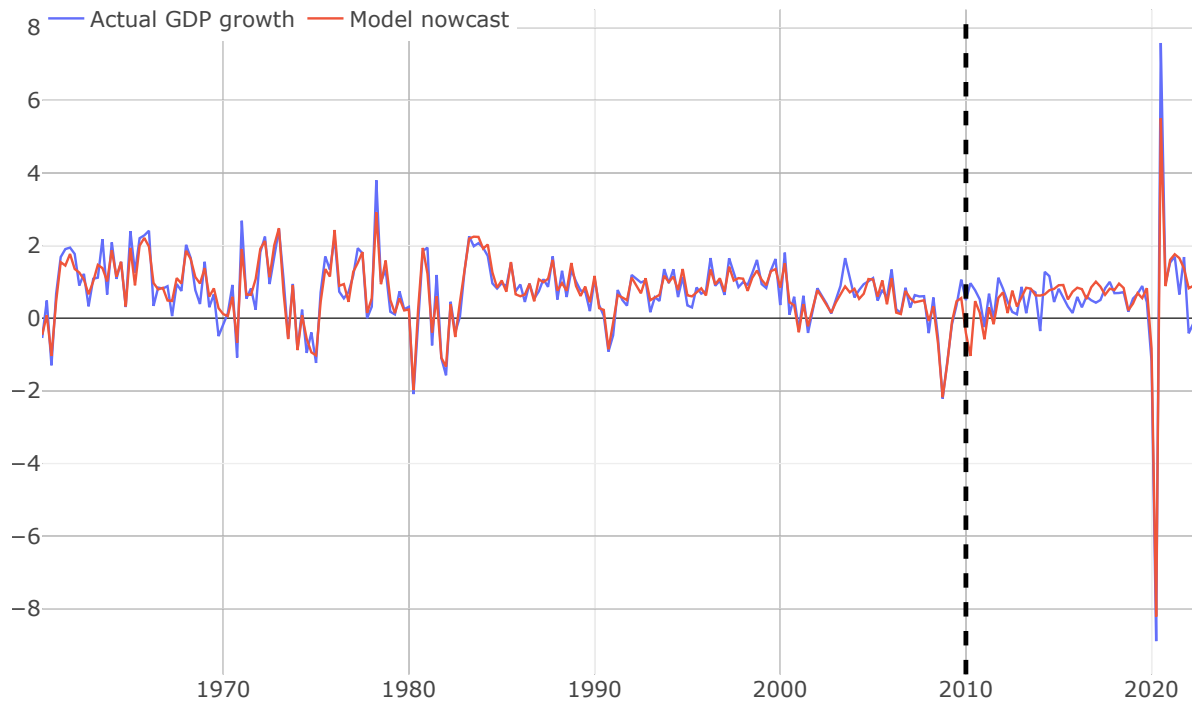
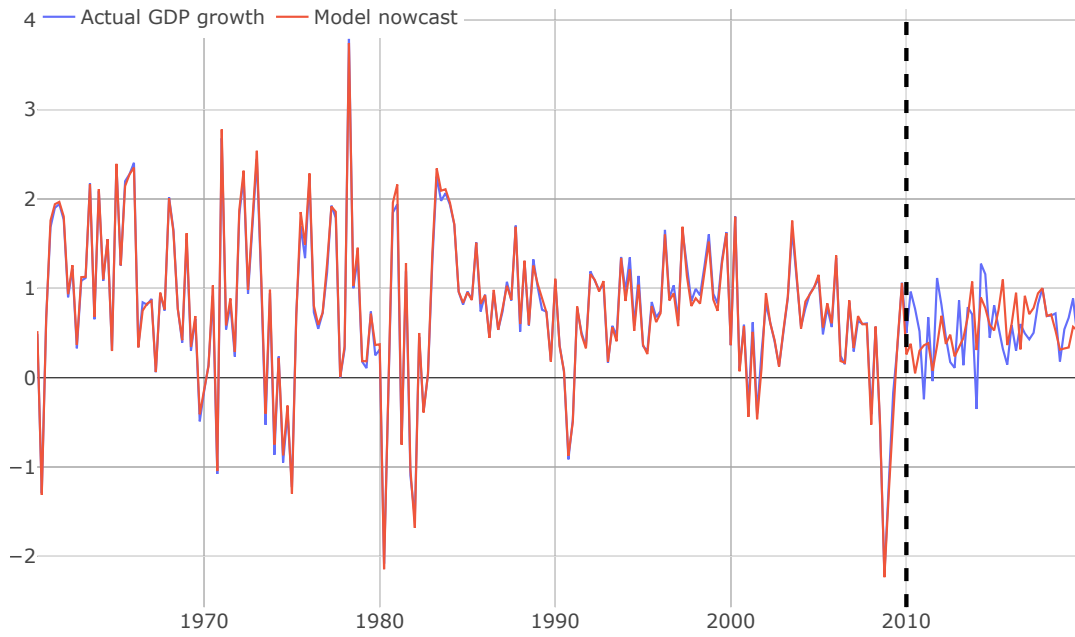
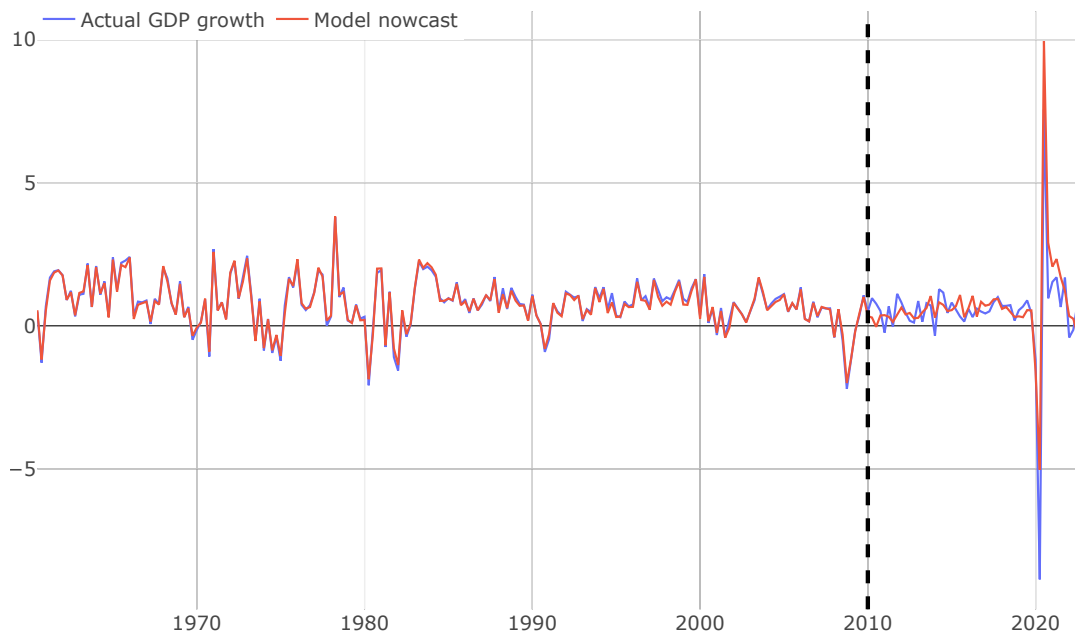


Figure 9: Nowcasting performance of the MLP ($n=16$, $l=4$). Evaluation period ranges from 2010:Q1 to 2022:Q3. Source: Own editing based on the FRED-MD database.

As we proposed, 1D CNN represents a “*sweet spot*” in terms of architectural design between the simple time-agnostic MLP and the more complex gated recurrent networks. Based on the results of Table 1 and Table 2, nowcasting performance of the 1D CNN seems very balanced as well. Although it does not achieve the best result in either of the two evaluation periods, its accuracy comes considerably close to that of the best model. Figure 10 below illustrates the nowcasting performance of the 1D CNN during our two evaluation periods.



(a) Nowcasting performance of the 1D CNN in the evaluation period without the COVID crisis (2010:Q1 – 2019:Q4).



(b) Nowcasting performance of the 1D CNN in the evaluation period including the COVID crisis (2010:Q1 – 2022:Q3)

Figure 10: Nowcasting performance of the 1D CNN ($n=16$, $l=8$). Source: Own editing based on the FRED-MD database.

5 Conclusion

In our study, we have conducted a nowcasting competition between different statistical models. The results of the empirical analysis show that all of our models can beat the naive benchmark model in terms of nowcasting performance. While the statistical significance of the performance gain changes between the different nowcasting scenarios, it is the strongest in the 3-month nowcasting scenario – as expected. So, the results clearly justify the use and relevance of this type of analysis. The results suggest that some properly selected neural network architectures can have even better nowcasting performance than the dynamic factor model, the state-of-the-art representative of traditional time-series approaches. We believe that our empirical analysis might indicate some important aspects of economic growth as well. Concretely, they can be expressive of the data-generating process of GDP growth. Previously, we have seen the results of two distinctively different evaluation periods. One is characterized by balanced economic growth, while the other also includes periods of the COVID-19 recession. The results show that longer input sequences result in more accurate nowcasts in periods of balanced economic growth. However, this effect ceases above a relatively low threshold value of around six quarters (eighteen months). During periods of economic turbulence (e.g., during the COVID-19 recession), longer sequences do not help the models’ predictive performance. Instead, they seem to weaken their generalization capability. Generally, the results suggest that long-term memory is not particularly relevant in the nowcasting of GDP growth. Our results show that 1D CNN, with the same weights, generates considerably accurate nowcasts in both of our evaluation periods. Consequently, first in the literature, we propose the use of this specific neural network architecture for economic nowcasting.

There remains much scope for future research and development on this topic. First, we plan to adopt a systematic (automated) procedure for feature selection. Sadly, as we know, gated RNNs do not have efficient filters and wrappers, similar to what was described in Crone and Kourentzes, 2010. In addition, a more systematic hyperparameter optimization routine could yield more accurate nowcasts and strengthen the conclusion of the empirical analysis.

References

- Bartholomew, D. J., Knott, M., & Moustaki, I. (2011). *Latent variable models and factor analysis: A unified approach*. John Wiley & Sons.
- Chernis, T., & Sekkel, R. (2017). A dynamic factor model for nowcasting Canadian GDP growth. *Empirical Economics*, *53*(1), 217–234.
- Chung, J., Gulcehre, C., Cho, K., & Bengio, Y. (2014). Empirical evaluation of gated recurrent neural networks on sequence modeling. *arXiv preprint arXiv:1412.3555*.
- Crone, S. F., & Kourentzes, N. (2010). Feature selection for time series prediction—A combined filter and wrapper approach for neural networks. *Neurocomputing*, *73*(10-12), 1923–1936.
- Dematos, G., Boyd, M. S., Kermanshahi, B., Kohzadi, N., & Kaastra, I. (1996). Feedforward versus recurrent neural networks for forecasting monthly japanese yen exchange rates. *Financial Engineering and the Japanese Markets*, *3*(1), 59–75.
- Diebold, F. X., & Mariano, R. S. (1995). Comparing Predictive Accuracy. *Journal of Business & Economic Statistics*, 253–263.
- Doz, C., Giannone, D., & Reichlin, L. (2011). A two-step estimator for large approximate dynamic factor models based on Kalman filtering. *Journal of Econometrics*, *164*(1), 188–205.
- Durbin, J., & Koopman, S. J. (2012). *Time series analysis by state space methods* (Vol. 38). OUP Oxford.
- Ekman, M. (2021). *Learning Deep Learning: Theory and Practice of Neural Networks, Computer Vision, NLP, and Transformers Using TensorFlow*. Addison-Wesley Professional.
- Ganesh, P. (2019). Types of Convolution Kernels: Simplified. <https://towardsdatascience.com/types-of-convolution-kernels-simplified-f040cb307c37>
- Giannone, D., Reichlin, L., & Small, D. (2008). Nowcasting: The real-time informational content of macroeconomic data. *Journal of monetary economics*, *55*(4), 665–676.
- Goodfellow, I., Bengio, Y., & Courville, A. (2016). *Deep Learning* [<http://www.deeplearningbook.org>]. MIT Press.
- Greene, W. H. (2017). *Econometric analysis* (Third). Pearson Education.
- Harvey, A. C. (1990). *Forecasting, structural time series models and the Kalman filter*. Cambridge university press.
- Heravi, S., Osborn, D. R., & Birchenhall, C. (2004). Linear versus neural network forecasts for European industrial production series. *International Journal of Forecasting*, *20*(3), 435–446.

- Hochreiter, S., & Schmidhuber, J. (1997). Long short-term memory. *Neural computation*, 9(8), 1735–1780.
- Hopp, D. (2021). Economic nowcasting with long short-term memory artificial neural networks (LSTM). *arXiv preprint arXiv:2106.08901*.
- Kiranyaz, S., Avci, O., Abdeljaber, O., Ince, T., Gabbouj, M., & Inman, D. J. (2021). 1D convolutional neural networks and applications: A survey. *Mechanical systems and signal processing*, 151, 107398.
- Kuan, C.-M., & Liu, T. (1995). Forecasting exchange rates using feedforward and recurrent neural networks. *Journal of applied econometrics*, 10(4), 347–364.
- Loermann, J., & Maas, B. (2019). Nowcasting US GDP with artificial neural networks.
- Marcellino, M., & Schumacher, C. (2010). Factor MIDAS for nowcasting and forecasting with ragged-edge data: A model comparison for German GDP. *Oxford Bulletin of Economics and Statistics*, 72(4), 518–550.
- Matheson, T. D. (2014). New indicators for tracking growth in real time. *OECD Journal: Journal of Business Cycle Measurement and Analysis*, 2013(2), 51–71.
- McCracken, M. W., & Ng, S. (2016). FRED-MD: A monthly database for macroeconomic research. *Journal of Business & Economic Statistics*, 34(4), 574–589.
- Olah, C. (2015). Understanding LSTM Networks. <http://colah.github.io/posts/2015-08-Understanding-LSTMs/>
- Schweppe, F. (1965). Evaluation of likelihood functions for Gaussian signals. *IEEE transactions on Information Theory*, 11(1), 61–70.
- Seabold, S., & Perktold, J. (2010). statsmodels: Econometric and statistical modeling with python. *9th Python in Science Conference*.
- Stock, J. H., & Watson, M. W. (2002). Forecasting using principal components from a large number of predictors. *Journal of the American statistical association*, 97(460), 1167–1179.
- Tkacz, G. (2001). Neural network forecasting of Canadian GDP growth. *International Journal of Forecasting*, 17(1), 57–69.
- Torres, D. G., & Qiu, H. (2018). Applying recurrent neural networks for multivariate time series forecasting of volatile financial data. *KTH Royal Institute of Technology: Stockholm, Sweden*.
- Wallis, K. F. (1986). Forecasting with an econometric model: The ‘ragged edge’ problem. *Journal of Forecasting*, 5(1), 1–13.

Appendix

The TCODE column denotes the following data transformation for a series x :

1. No transformation
2. Δx_t
3. $\Delta^2 x_t$
4. $\log(x_t)$
5. $\Delta \log(x_t)$
6. $\Delta^2 \log(x_t)$
7. $\Delta \left(\frac{x_t - x_{t-1}}{x_{t-1}} \right)$

The FRED column gives mnemonics in FRED followed by a short description. Some series require adjustments to the raw data available in FRED. These variables are tagged by an asterisk to indicate that they have been adjusted and thus differ from the series from the source. For a detailed summary of the adjustments see McCracken and Ng, 2016.

Group 1: Output and income

	ID	tcode	FRED	Description
1	1	5	RPI	Real Personal Income
2	2	5	W875RX1	Real personal income ex transfer receipts
3	6	5	INDPRO	IP Index
4	7	5	IPFPNSS	IP: Financial Products and Nonindustrial Supplies
5	8	5	IPFINAL	IP: Final Products (Market Group)
6	9	5	IPCONGD	IP: Consumer Goods
7	10	5	IPDCONGD	IP: Durable Consumer Goods
8	11	5	IPNCONGD	IP: Nondurable Consumer Goods
9	12	5	IPBUSEQ	IP: Business Equipment
10	13	5	IPMAT	IP: Materials
11	14	5	IPDMAT	IP: Durable Materials
12	15	5	IPNMAT	IP: Nondurable Materials
13	16	5	IPMANSICS	IP: Manufacturing (SIC)
14	17	5	IPB51222s	IP: Residential Utilities
15	18	5	IPFUELS	IP: Fuels
16	19	1	NAPMPI	ISM Manufacturing: Production Index
17	20	2	CUMFNS	Capacity Utilization: Manufacturing

Group 2: Labor market

ID	tcode	FRED	Description	
1	21*	2	HWI	Help-Wanted Index for United States
2	22*	2	HWIURATIO	Ratio of Help Wanted/No. Unemployed
3	23	5	CLF160OV	Civilian Labor Force
4	24	5	CE160V	Civilian Employment
5	25	2	UNRATE	Civilian Unemployment Rate
6	26	2	UEMPMEAN	Average Duration of Unemployment (Weeks)
7	27	5	UEMPLT5	Civilians Unemployed – Less Than 5 Weeks
8	28	5	UEMP5TO14	Civilians Unemployed for 5-14 Weeks
9	29	5	UEMP15OV	Civilians Unemployed – 15 Weeks and Over
10	30	5	UEMP15T26	Civilians Unemployed for 15 – 26 Weeks
11	31	5	UEMP27OV	Civilians Unemployed for 27 Weeks and Over
12	32*	5	CLAIMSx	Initial Claims
13	33	5	PAYEMS	All Employees: Total nonfarm
14	34	5	USGOOD	All Employees: Goods-Producing Industries
15	35	5	CES1021000001	All Employees: Mining and Logging: Industries
16	36	5	USCONS	All Employees: Construction
17	37	5	MANEMP	All Employees: Manufacturing
18	38	5	DMANEMP	All Employees: Durable Goods
19	39	5	NDMANEMP	All Employees: Nondurable Goods
20	40	5	SRVPRD	All Employees: Service-Providing Industries
21	41	5	USTPU	All Employees: Trade, Transportation and Utilities
22	42	5	USWTRADE	All Employees: Wholesale Trade
23	43	5	USTRADE	All Employees: Retail Trade
24	44	5	USFIRE	All Employees: Financial Activities
25	45	5	USGOVT	All Employees: Government
26	46	1	CES0600000007	Avg Weekly Hours: Goods-Producing
27	47	2	AWOTMAN	Avg Weekly Overtime Hours: Manufacturing
28	48	1	AWHMAN	Avg Weekly Hours: Manufacturing
29	49	1	NAPMEI	ISM Manufacturing: Employment Index
30	127	6	CES0600000008	Avg Hourly Earnings: Goods-Producing
31	128	6	CES2000000008	Avg Hourly Earnings: Construction
32	129	6	CES3000000008	Avg Hourly Earnings: Manufacturing

Group 3: Housing

ID	tcode	FRED	Description	
1	50	4	HOUST	Housing Starts: Total New Privately Owned
2	51	4	HOUSTNE	Housing Starts: Northeast
3	52	4	HOUSTMW	Housing Starts: Midwest
4	53	4	HOUSTS	Housing Starts: South
5	54	4	HOUSTW	Housing Starts: West
6	55	4	PERMIT	New Private Housing Permits (SAAR)
7	56	4	PERMITNE	New Private Housing Permits: Northeast (SAAR)
8	57	4	PERMITMW	New Private Housing Permits: Midwest (SAAR)
9	58	4	PERMITS	New Private Housing Permits: South (SAAR)
10	59	4	PERMITW	New Private Housing Permits: West (SAAR)

Group 4: Consumption, orders and inventories

ID	tcode	FRED	Description	
1	3	5	DPCERA3M086SBEA	Real personal consumption expenditures
2	4*	5	CMRMTSPLx	Real Manu. and Trade Industries Sales
3	5*	5	RETAILx	Retail and Food Services Sales
4	60	1	NAPM	ISM: PMI Composite Index
5	61	1	NAPMNOI	ISM: New Orders Index
6	62	1	NAPMSDI	ISM: Supplier Deliveries Index
7	63	1	NAPMII	ISM: Inventories Index
8	64	5	ACOGNO	New Orders for Consumer Goods
9	65*	5	AMDMMNOx	New Orders for Durable Goods
10	66*	5	ANDENOX	New Orders for Nondefense Capital Goods
11	67*	5	AMDMMUOX	Unfilled Orders for Durable Goods
12	68*	5	BUSINVx	Total Business Inventories
13	69*	2	ISRATIOx	Total Business: Inventories to Sales Ratio
14	130*	2	UMSCENTx	Consumer Sentiment Index

Group 5: Money and credit

ID	tcode	FRED	Description	
1	70	6	M1SL	M1 Money Stock
2	71	6	M2SL	M2 Money Stock
3	72	5	M2REAL	Real M2 Money Stock
4	73	6	AMBSL	St. Louis Adjusted Monetary Base
5	74	6	TOTRESNS	Total Reserves of Depository Institutions
6	75	7	NONBORRES	Reserves of Depository Institutions
7	76	6	BUSLOANS	Commercial and Industrial Loans
8	77	6	REALLN	Real Estate Loans at All Commercial Banks
9	78	6	NONREVSL	Total Nonrevolving Credit
10	79*	2	CONSPI	Nonrevolving consumer credit to Personal Income
11	131	6	MZMSL	MZM Money Stock
12	132	6	DTCOLNVHFNM	Consumer Motor Vehicle Loans Outstanding
13	133	6	DTCTHFNM	Total Consumer Loans and Leases Outstanding
14	134	6	INVEST	Securities in Bank Credit at All Commercial Banks

Group 6: Interest and exchange rates

ID	tcode	FRED	Description
1	84	2	FEDFUNDS Effective Federal Funds Rate
2	85*	2	CP3Mx 3-Month AA Financial Commercial Paper Rate
3	86	2	TB3MS 3-Month Treasury Bill
4	87	2	TB6MS 6-Month Treasury Bill
5	88	2	GS1 1-Year Treasury Rate
6	89	2	GS5 5-Year Treasury Rate
7	90	2	GS10 10-Year Treasury Rate
8	91	2	AAA Moody's Seasoned Aaa Corporate Bond Yield
9	92	2	BAA Moody's Seasoned Baa Corporate Bond Yield
10	93*	1	COMPAPFFx 3-Month Commercial Paper Minus FEDFUNDS
11	94	1	TB3SMFFM 3-Month Treasury C Minus FEDFUNDS
12	95	1	TB6SMFFM 6-Month Treasury C Minus FEDFUNDS
13	96	1	T1YFFM 1-Year Treasury C Minus FEDFUNDS
14	97	1	T5YFFM 5-Year Treasury C Minus FEDFUNDS
15	98	1	T10YFFM 10-Year Treasury C Minus FEDFUNDS
16	99	1	AAAFFM Moody's Aaa Corporate Bond Minus FEDFUNDS
17	100	1	BAAFFM Moody's Baa Corporate Bond Minus FEDFUNDS
18	101	5	TWEXMMTH Trade Weighted U.S. Dollar Index: Major Currencies
19	102*	5	EXSZUSx Switzerland / U.S. Foreign Exchange Rate
20	103*	5	EXJPUSx Japan / U.S. Foreign Exchange Rate
21	104*	5	EXUSUKx U.S. / U.K. Foreign Exchange Rate
22	105*	5	EXCAUSx Canada / U.S. Foreign Exchange Rate

Group 7: Prices

ID	tcode	FRED	Description	
1	106	6	WPSFD49207	PPI: Finished Goods
2	107	6	WPSFD49502	PPI: Finished Consumer Goods
3	108	6	WPSID61	PPI: Intermediate Materials
4	109	6	WPSID62	PPI: Crude Materials
5	110*	6	OILPRICE _x	Crude Oil, spliced WTI and Cushing
6	111	6	PPICMM	PPI: Metals and metal products
7	112	1	NAPMPRI	ISM Manufacturing: Prices Index
8	113	6	CPIAUCSL	CPI: All Items
9	114	6	CPIAPPSL	CPI: Apparel
10	115	6	CPITRNSL	CPI: Transportation
11	116	6	CPIMEDSL	CPI: Medical Care
12	117	6	CUSR0000SAC	CPI: Commodities
13	118	6	CUSR0000SAD	CPI: Durables
14	119	6	CUSR0000SAS	CPI: Service
15	120	6	CPIULFSL	CPI: All Items less Food
16	121	6	CUSR0000SA0L2	CPI: All Items less Shelter
17	122	6	CUSR0000SA0L5	CPI: All Items less Medical Care
18	123	6	PCEPI	Personal Cons. Expend.: Chain Index
19	124	6	DDURRG3M086SBEA	Personal Cons. Expend.: Durable Goods
20	125	6	DNDGRG3M086SBEA	Personal Cons. Expend.: Nondurable Goods
21	126	6	DSERRG3M086SBEA	Personal Cons. Expend.: Services

Group 8: Stock market

ID	tcode	FRED	Description	
1	80*	5	S&P 500	S&P's Common Stock Price Index: Composite
2	81*	5	S&P: indust	S&P's Common Stock Price Index: Industrials
3	82*	2	S&P div yield	S&P's Composite Common Stock: Dividend Yield
4	83*	5	S&P PE ratio	S&P's Composite Common Stock: Price-Earnings Ratio